BULLETIN OF THE EARTHQUAKE
RESEARCH INSTITUTE
Vol. 45 (1967), pp. 657-678

# 35. *Upper Mantle Structure from Apparent Velocities of P Waves Recorded at Wakayama Micro-Earthquake Observatory.*

By Hiroo KANAMORI,

Earthquake Research Institute.

(Read April 25, 1967.—Received June 30, 1967.)

## Abstract

Direct measurements of apparent velocities, $d\Delta/dt$, of $P$ waves are made for about fifty earthquakes recorded at Wakayama Micro-Earthquake Observatories for the distance range 5° to 55°. The main features of the variation of $d\Delta/dt$ are as follows. $d\Delta/dt \fallingdotseq 8.0$ km/sec ($5° < \Delta < 12°$), $d\Delta/dt \fallingdotseq 8.8$ km/sec ($15° < \Delta < 19°$), $d\Delta/dt \fallingdotseq 12.8$ to 13.0 km/sec ($27° < \Delta < 40°$). The transition from the 8 km/sec branch to the 8.8 km/sec branch is relatively abrupt. A clear discontinuous change of $d\Delta/dt$ is observed at $\Delta = 19.3°$, followed by a rapid increase from 9.8 to 12.5 km/sec up to $\Delta = 25°$. Amplitude becomes very small around $\Delta = 15°$, and at $16° < \Delta < 22°$ a large later phase is observed. To explain the observed apparent velocity data, a preliminary velocity-depth model with the following major features is derived. The velocity is almost constant, about 7.9 km/sec, down to 150 km depth where it rapidly increases to 8.3 km/sec. Another rapid velocity increase starts at the depth of 375 km. Below 430 km the velocity variation with depth is midway between those of the Jeffreys and the CIT11CS3 models. Travel-time residual from the Jeffreys-Bullen Table for the preliminary model is consistent with those determined by explosion and earthquake studies. The velocity increase at the depth of 150 km is difficult to explain by a simple pressure and temperature effect on a homogeneous mantle. Compositional change or partial melting or both may have to be invoked. The rapid velocity increase at the depth of 375 km is in good harmony with the idea of the olivine-spinel transition of $(Mg, Fe)_2SiO_4$. The temperature at this level can be estimated as 1300 to 1500°C for a reasonable composition of the mantle. Earthquake energy release which takes a maximum value at this level in the Japan region may be attributed to the same cause and may have an important bearing on island arc tectonics.

## § 1. Introduction

The most reliable and fundamental knowledge of the earth's interior has been supplied by seismic travel-time studies. Recent reviews by *Nuttli* [1963], *Anderson* [1965, 1967a], and *Savarenskii* [1966] describe the present situation. A number of different structures are reported by different studies for different regions. A part of these differences is undoubtedly due to a regional effect, particularly in the upper mantle. Although the travel-time studies are very useful in determining general features of the velocity distribution with depth, it is extremely difficult to determine detailed structures, since the inevitable smoothing of travel-time data obscures details considerably. This seems to be partly reflected in the differences reported hitherto. Direct measurement of the apparent velocities $d\Delta/dt$ has a great advantage in this respect over the ordinary travel-time method. *Niazi and Anderson* [1965] applied the apparent velocity method to elucidate structural details. Although the scatter of their data is large, they found relatively sharp velocity increases at the depths of 320 and 640 km. *Johnson* [1967] made array measurements of $P$ waves for the basin and range province in the Western United States and succeeded in revealing a detailed upper mantle structure. *Chinnery and Toksöz* [1967] studied the lower mantle structure by the apparent velocities measured at the Lasa array in Montana.

Another advantage of the apparent velocity method is that there is little difficulty in adding up data from a number of different earthquakes. The "source correction" due to the regionality of the source, and the errors in hypocenter determinations have little effect in the apparent velocity determination. Both of these seriously affect the usual travel-time method. The purpose of the present work is to study structural details in the upper mantle around Japan by using the apparent velocity method. For a precise measurement of apparent velocities, seismometer arrays with identical seismographs and of a considerable linear dimension are most suited. None of these exists in Japan at present. However, Wakayama Micro-Earthquake Observatory and its substations operated by the Earthquake Research Institute of the University of Tokyo can meet many of the essential requirements for the precise measurements of apparent velocities. Details of the Wakayama Observatories are published in Seismological Bulletin of the Observatory [*Wakayama Micro-Earthquake Observatory*, 1966]. The location map

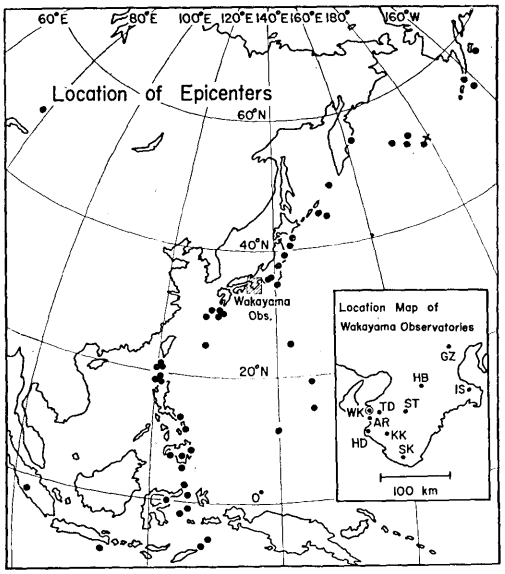


Fig. 1. Location of epicenters and Wakayama Micro-Earthquake Observatories. Station names (abbreviation) and detailed locations are given in the insert. A cross mark is the underground nuclear explosion Long Shot.

and abbreviated station names are given in the insert of Figure 1. All the stations are equipped with short-period seismometers having a peak displacement response at 20 cps. The displacement magnification varies from one station to another, ranging from 5500 to 18000 at 1 cps. Recordings are made with a paper speed of 4 mm/sec on a drum recorder equipped with an ink-writing galvanometer and a 1 sec time marker. The maximum extent of the station net is about 1.5° and the minimum is 0.8°. The linear dimension of about 1° distance seems appropriate for the direct measurement of the apparent velocity. If the extent is too small, the reading error and the station anomalies greatly disturb the measurement. If the linear dimension of the net is too large, fine structures of the $d\Delta/dt$ curve may be overlooked.

## § 2. Data

About fifty earthquakes selected from the observatory bulletin for the interval January 1965 to June 1965 are studied. The records of the Long Shot underground nuclear explosion of Oct. 29, 1965 and one Kuril earthquake of Dec. 30, 1963 are added for supplementary use (Table 1). The epicenter locations are given in Figure 1.

The hypocenter data are supplied from the Preliminary Determination of Epicenter (PDE) published by the United States Coast and Geodetic Survey (USCGS).

## § 3. Analysis

The distances $\Delta$ are calculated on the basis of the PDE of USCGS. To reduce $\Delta$ for all the earthquakes to that for corresponding normal

Table 1. List of earthquakes for which $d\Delta/dt$ is measured. C. Delta is distance corrected for focal depth. $C$ is $d\Delta/dt$ in km/sec.

| Date | Year | O.T.(GST) h m s | Depth (km) | MAG | Azim (Deg) | Delta (Deg) | C. Delta (Deg) | C (km/sec) |
|---|---|---|---|---|---|---|---|---|
| JAN02 | 65 | 13 44 18 9 | 142 | 6.1 | 148 | 17.31 | 18.55 | 8.70 |
| JAN07 | 65 | 18 49 35 0 | 33 | 4.8 | 224 | 20.40 | 20.40 | 10.04 |
| JAN09 | 65 | 13 32 46 4 | 5 | 6.1 | 204 | 23.74 | 23.57 | 11.14 |
| JAN11 | 65 | 09 44 58 3 | 33 | 4.9 | 230 | 6.19 | 6.19 | 7.99 |
| JAN11 | 65 | 22 47 06 3 | 102 | 5.0 | 37 | 19.71 | 20.61 | 9.82 |
| JAN14 | 65 | 01 33 14 6 | 140 | 5.3 | 237 | 6.93 | 11.81 | 7.92 |
| JAN15 | 65 | 05 59 58 5 | 0 | 6.3 | 309 | 44.00 | 43.85 | 14.08 |
| JAN23 | 65 | 21 51 14 9 | 58 | 5.1 | 56 | 4.99 | 6.57 | 7.87 |
| JAN24 | 65 | 00 11 12 1 | 6 | 6.6 | 196 | 37.34 | 37.22 | 12.84 |
| JAN28 | 65 | 02 34 03 0 | 33 | 5.6 | 227 | 47.89 | 47.89 | 15.02 |
| FEB04 | 65 | 12 06 04 3 | 25 | 5.8 | 44 | 31.91 | 31.86 | 12.18 |
| FEB05 | 65 | 09 32 09 3 | 41 | 5.9 | 45 | 32.91 | 32.96 | 12.81 |
| FEB06 | 65 | 01 40 33 2 | 33 | 6.4 | 47 | 47.42 | 47.42 | 14.02 |
| FEB15 | 65 | 10 43 19 8 | 33 | 6.0 | 199 | 32.24 | 32.24 | 12.72 |
| FEB16 | 65 | 12 24 08 8 | 33 | 5.6 | 41 | 7.30 | 7.30 | 7.90 |
| FEB27 | 65 | 02 01 36 3 | 33 | 5.2 | 218 | 10.99 | 10.99 | 7.95 |
| MAR01 | 65 | 08 18 56 4 | 42 | 5.2 | 228 | 18.34 | 18.44 | 8.76 |
| MAR01 | 65 | 13 20 56 7 | 42 | 5.5 | 229 | 18.26 | 18.36 | 8.80 |
| MAR11 | 65 | 08 31 01 3 | 49 | 4.5 | 41 | 16.03 | 16.38 | 8.71 |
| MAR19 | 65 | 22 58 34 9 | 173 | 5.6 | 201 | 35.80 | 36.85 | 12.64 |
| MAR21 | 65 | 11 08 16 2 | 33 | 6.2 | 195 | 36.32 | 36.32 | 12.80 |
| MAR24 | 65 | 22 42 09 6 | 51 | 5.8 | 200 | 26.79 | 26.94 | 12.20 |
| MAR28 | 65 | 13 22 57 6 | 33 | 5.9 | 33 | 27.95 | 27.95 | 12.71 |
| MAR29 | 65 | 10 47 37 6 | 33 | 6.1 | 38 | 8.78 | 8.78 | 7.95 |
| MAR30 | 65 | 02 27 07 2 | 51 | 5.7 | 49 | 34.76 | 34.82 | 13.00 |
| APR05 | 65 | 13 52 13 4 | 81 | 5.7 | 44 | 15.86 | 16.71 | 8.63 |
| APR06 | 65 | 05 31 59 7 | 69 | 5.7 | 58 | 3.78 | 6.12 | 8.09 |
| APR12 | 65 | 15 50 37 9 | 40 | 4.9 | 61 | 3.96 | 4.93 | 8.05 |
| APR24 | 65 | 08 02 26 3 | 43 | 5.0 | 225 | 19.63 | 19.70 | 10.40 |
| APR24 | 65 | 21 55 26 5 | 59 | 5.7 | 169 | 22.77 | 23.02 | 11.30 |
| APR25 | 65 | 01 00 11 6 | 15 | 5.6 | 145 | 11.33 | 11.15 | 8.10 |
| APR25 | 65 | 21 28 40 5 | 28 | 4.9 | 224 | 6.08 | 6.07 | 7.95 |
| APR26 | 65 | 20 29 07 4 | 53 | 5.9 | 45 | 47.11 | 47.22 | 14.34 |
| APR26 | 65 | 22 15 42 5 | 33 | 5.9 | 229 | 18.46 | 18.46 | 8.70 |
| APR27 | 65 | 10 54 28 0 | 67 | 5.9 | 190 | 41.12 | 41.35 | 12.95 |
| MAY07 | 65 | 02 29 03 9 | 57 | 4.9 | 154 | 21.90 | 22.10 | 11.00 |
| MAY08 | 65 | 03 05 38 5 | 56 | 5.6 | 225 | 20.94 | 21.14 | 10.59 |
| MAY16 | 65 | 11 35 46 0 | 36 | 6.2 | 200 | 30.17 | 30.17 | 12.89 |
| MAY18 | 65 | 12 08 51 4 | 34 | 4.8 | 235 | 8.02 | 8.02 | 7.80 |
| MAY22 | 65 | 03 05 43 6 | 25 | 5.5 | 197 | 33.80 | 33.76 | 12.57 |
| MAY23 | 65 | 23 46 12 0 | 22 | 6.1 | 45 | 33.24 | 33.18 | 12.80 |
| MAY24 | 65 | 05 02 11 8 | 67 | 5.0 | 211 | 48.31 | 48.51 | 14.70 |
| MAY24 | 65 | 23 21 10 6 | 33 | 5.9 | 208 | 23.34 | 23.34 | 11.40 |
| MAY31 | 65 | 11 38 28 0 | 37 | 6.0 | 190 | 41.80 | 41.80 | 12.80 |
| JUN13 | 65 | 07 06 10 2 | 20 | 5.7 | 38 | 9.70 | 9.55 | 8.44 |
| JUN18 | 65 | 22 58 14 7 | 51 | 4.9 | 85 | 4.51 | 5.74 | 8.04 |
| JUN22 | 65 | 23 48 07 1 | 60 | 5.6 | 205 | 29.08 | 29.28 | 12.71 |
| JUN23 | 65 | 11 09 15 3 | 36 | 5.7 | 42 | 52.46 | 52.46 | 15.42 |
| JUN24 | 65 | 07 45 13 6 | 50 | 6.0 | 200 | 28.25 | 28.39 | 13.30 |
| JUN26 | 65 | 16 47 50 7 | 34 | 4.8 | 227 | 6.36 | 6.36 | 8.18 |
| OCT29 | 65 | 21 00 00 1 | 1 | 5.5 | 48 | 35.80 | 35.65 | 12.85 |

earthquakes ($d=33$ km), corrections in $\Delta$ are made for earthquakes having focal depths other than 33 km, based on the Jeffreys-Bullen Table. Only minor differences result from a different choice of the travel-time table for this correction. Travel times are calculated from the observed arrival times of $P$ and the reported origin times, station height corrections and ellipticity corrections being subtracted. The calculations of $d\Delta/dt$ were first made only from the reported times in the Bulletin. The results were generally coherent but a much better result was obtained when original seismograms from all the stations were copied and pasted up.

The apparent velocities $d\Delta/dt$ for about one half of the earthquakes are determined by referring to the original records. Several examples are given in Figures 2, 3, 4, 5, 6, and 7. The record of each station is displaced along the time axis proportionally to the epicenter distance of the station, so that all the traces are aligned approximately vertically.

Straight lines corresponding to three apparent velocities are drawn in the figures from which it is seen that the uncertainty of the $d\Delta/dt$ determinations is much less than $\pm 0.5$ km/sec under favorable conditions. The apparent velocities thus determined are listed in Table 1 and shown in Figure 8 with different marks for different azimuths. Data for NW and SE directions are very few (1 for NW, 4 for SE), but no large

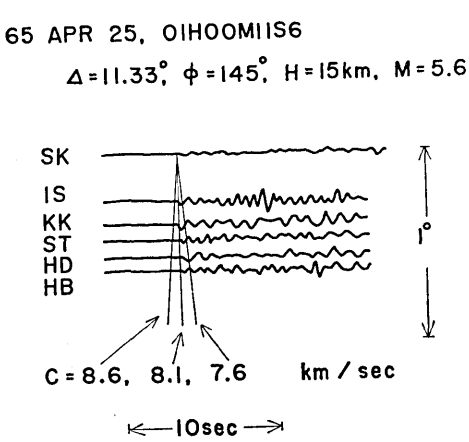


Fig. 2. Seismograms at $\Delta=11.33°$.

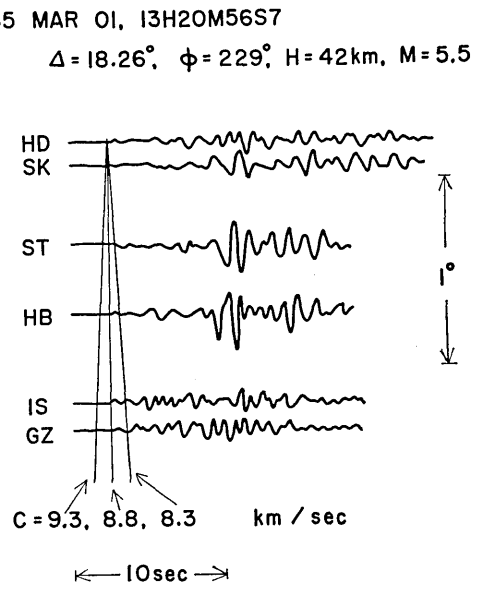


Fig. 3. Seismograms at $\Delta=18.26°$.

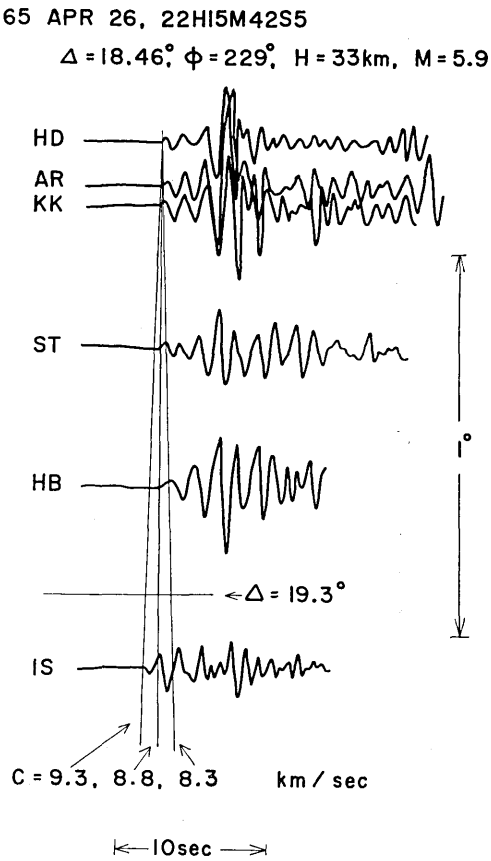


Fig. 4. Seismograms at $\Delta=18.64°$. Seismogram at IS shows a commencement of a large first arrival.

difference is observed as far as the present data are concerned.

A dipping interface below the station net systematically affects the measurement of the apparent velocity. *Niazi* [1966] calculated the effect for a single interface model and tabulated the results in a convenient form. Although no seismic determination of the dip of the Moho has been made, the regional distribution of Bouguer gravity anomalies suggests that the Moho dips considerably towards the north, though not more than 2°. Assuming that the ratio of the crustal to mantle velocities is 0.8, it immediately follows from Niazi's Table 4A that, for $\Delta \leqq 50°$ ($I \geqq 25°$), the error in $d\Delta/dt$ is smaller than 2 per cent, which is less than the observation error. Circled values in Figure 8 indicate reliable data obtained from seismograms which show very sharp onsets.

The apparent velocity is almost constant up to $\Delta=12°$. The amplitude becomes very small towards $\Delta=14°$. From $\Delta=15°$ to 19° the velocity is around 8.8 km/sec. The transition from 8 to 8.8 km/sec appears relatively abrupt although no reliable determinations of $d\Delta/dt$ could be made because of the diminution of the amplitude. Over this range a large later phase is observed, two examples of which will be discussed later. At $\Delta=19.3°$, a discontinuous change in the apparent velocity is observed. A very rapid increase of the velocity follows up to $\Delta=23°$. At $27° < \Delta < 40°$, the apparent velocity is nearly constant. At distances larger than 43°, the increase of $d\Delta/dt$ is fairly rapid although the measurement becomes less reliable at larger distances because of the decrease of the total delay time within the net

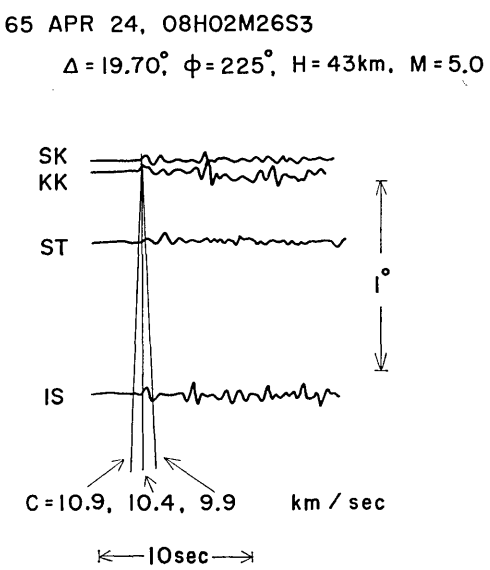


Fig. 5. Seismograms at $\Delta$=19.70°.

and of the dipping Moho.

## § 4. Supplementary data

The Herglotz-Wiechert method is applicable to the determination of the velocity structure, if we know apparent velocities for all possible branches of travel-time curves. The present determination of the apparent velocity is limited only to the first arrivals. It is, therefore, not possible to determine a unique velocity-depth function within the earth's mantle, even if low-velocity zones can be appropriately taken care of by the method of successive stripping. To reduce the ambiguities of the interpretation, amplitude variations with distance, later phases, and travel times are considered.

Although quantitative determination of the amplitude variation with

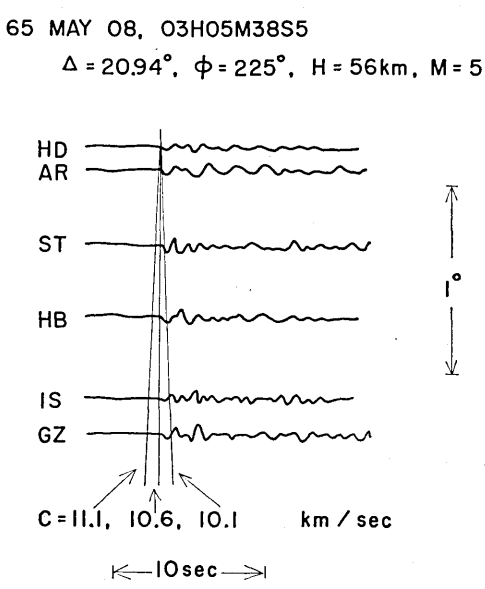


Fig. 6. Seismograms at $\Delta$=20.94°.

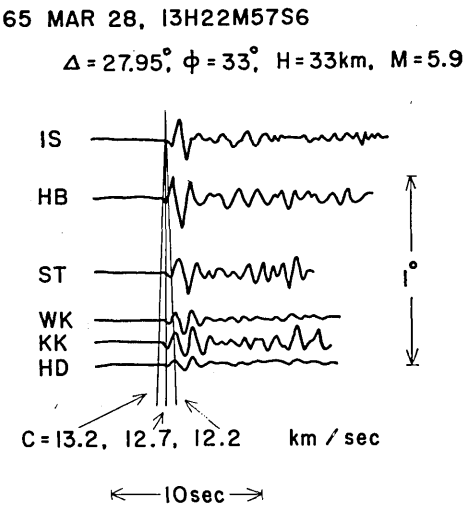


Fig. 7. Seismograms at $\Delta$=27.95°.

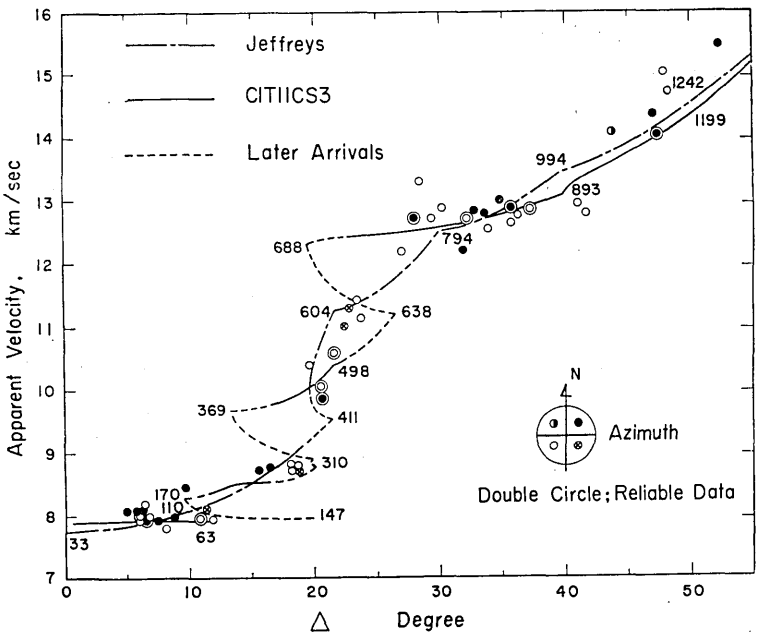


Fig. 8. Observed apparent velocities versus distance. Solid and broken curves are for the CIT11CS3 and Jeffreys models given in Figure 13. Dotted curves indicate later phase branches. Numbers indicate the depths of penetration of the rays.

distance is not made here, we observed no clear indication of shadow zones. However, it is observed that the amplitude of the first arrival is sometimes very small around $\Delta=14°$. *Kishimoto* [1956] first found this trend for Japanese earthquakes using records of the Japan Meteorological Agency (JMA) stations. He also found a relatively large later phase emerging at $\Delta=13°$ several seconds after the first arrival. A similar feature is often found in the present study though at slightly larger distances. Figure 9 shows seismograms of a Kuril earthquake recorded at closely located stations at distances

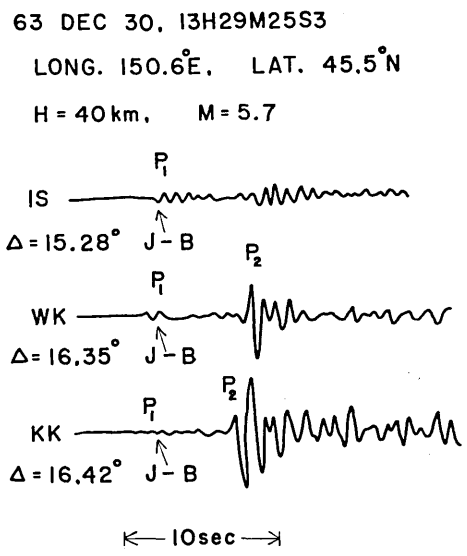


Fig. 9. Seismograms showing large later arrivals emerging at $\Delta=16°$. Arrivals at the J-B times are small.

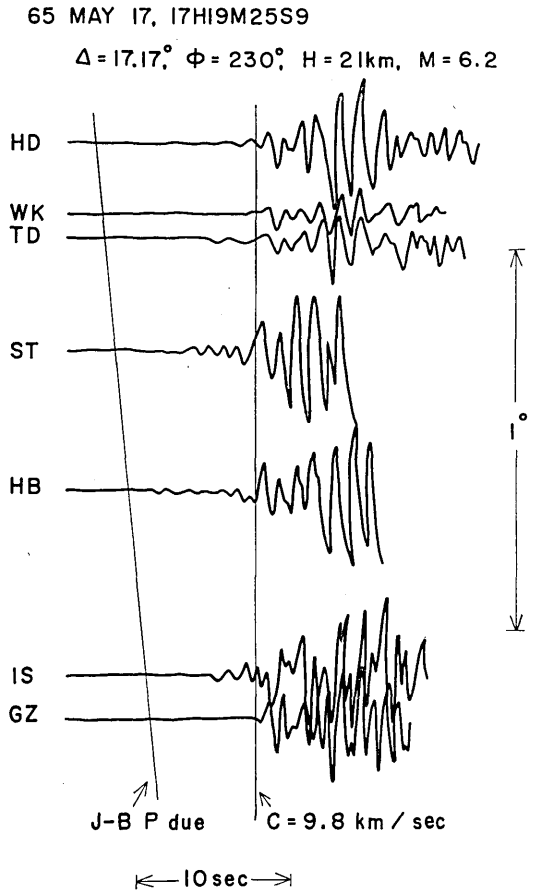


Fig. 10. Seismograms at $\Delta=17.17°$. Commencement of the $P$ phase is not clear. Two lines corresponding to J-B time and $C=9.8$ km/sec are drawn only for reference.

around 16°. A large later phase designated as $P_2$ which is not very clear at station IS ($\Delta=15.28°$) emerges at stations WK ($\Delta=16.35°$) and KK ($\Delta=16.42°$). Figure 10 shows another set of seismograms at distances around 17°. Arrivals at the Jeffreys-Bullen times are not clear, but relatively large phases are observed a few seconds later, though some of these later phases may be due to multiple shocks. Supplementary data from JMA stations also suggest this. Figure 11 is a composite presentation of travel times of four earthquakes. The difference of the observed travel times from the Jeffreys-Bullen times corresponding to the focal depth of each earthquake is plotted. Hypocenter data given by USCGS are used for the calculation of the distances and travel times. Except at $14°<\Delta<22°$ and $\Delta<5°$, the difference is, on an average, within $\pm 2$ seconds. A clear delayed branch extending from $\Delta=16°$ to $\Delta=22°$ is observed for the earthquake of May 17, 1965. JMA reports only first arrivals but the magnification is not high enough to record weak arrivals. This branch is therefore quite likely to be of later arrivals, weak first arrivals being overlooked. Actually, a branch which seems to represent the first arrivals is observed for the earthquake of June 11, 1965. This delayed branch as evidenced by Figures 9, 10, and 11 is probably the same as that observed by Kishimoto. *Archambeau et al.* [1966] also found this branch and

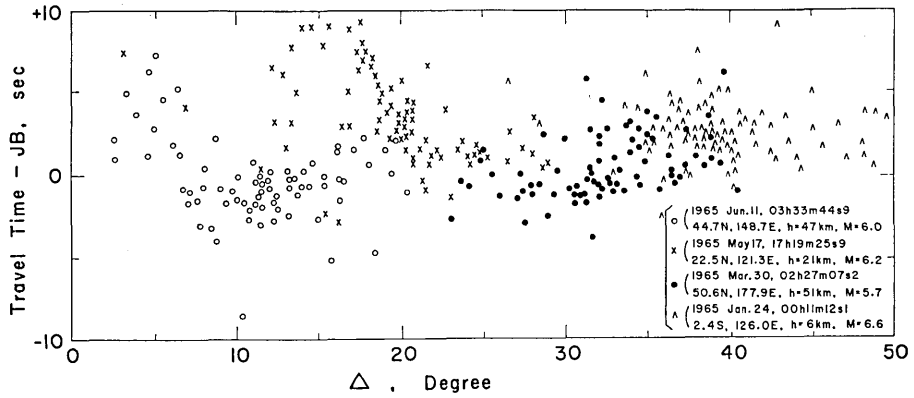


Fig. 11. Composite travel times for four different earthquakes recorded at the Japan Meteorological Agency Stations. The ordinate shows the residuals from the J-B Table. Positive and negative times indicate late and early arrivals respectively.

designated it as $P_2$. This branch can be interpreted as due to a strong upward refraction by a sharp velocity increase with depth.

Travel times are also calculated from the USCGS hypocenter data for the earthquakes listed in Table 1. Since the earthquakes are of different focal depths, appropriate corrections in distances and travel times are made to reduce the depths to 33 km ($h=0.00\,r_0$). The Jeffreys-Bullen Table is used for this correction. Reduced travel times $T-13.6\Delta$ are plotted in Figure 12 as compared with the Jeffreys-Bullen curve for $h=0.00\,r_0$. The large scatter at distances $\Delta<20°$ is probably due to differences in the structure of the hypocentral area of each earthquake. The Jeffreys-Bullen curve explains well the average features of the observed travel times, although the accuracy of the USCGS hypocenter location may be questioned for quantitative discussions of absolute travel times.

## § 5. Construction of velocity-depth model

In what follows we will construct a velocity-depth model which best explains the observed apparent velocity data. Other supplementary features such as the frequently observed small amplitude of the first arrival at $\Delta=14°$, and the strong later phase branch at $16°<\Delta<22°$ (Figures 9, 10, and 11) will be considered in an approximate manner. We will start with two velocity models, the Jeffreys model and the CIT11CS3 model [*Niazi and Anderson*, 1965] which is a smoothed version of the CIT11 model introduced by *Anderson and Toksöz* [1963]. The

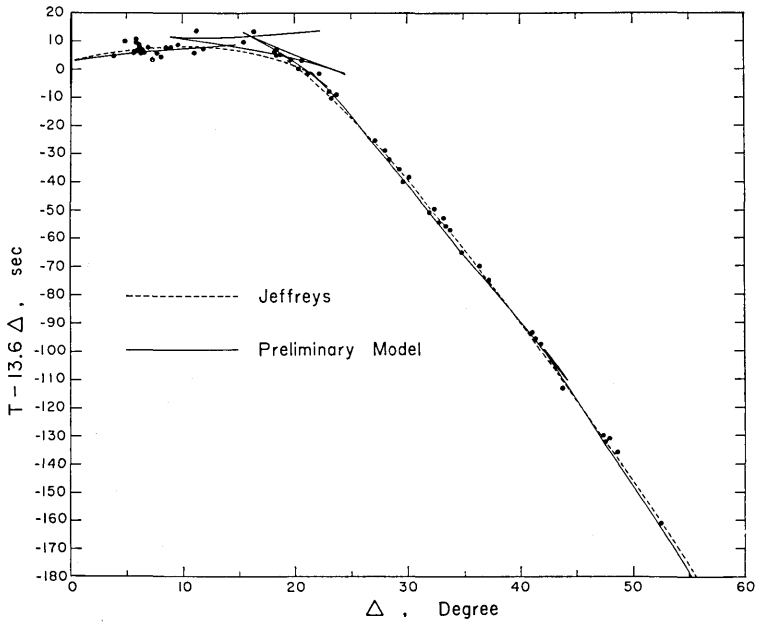


Fig. 12. Reduced travel times as compared with the Jeffreys and the preliminary velocity structures given in Figure 13.

models are shown in Figure 13 and Table 2, and the corresponding apparent velocities in Figure 8.

The constancy of the apparent velocity of about 8 km/sec up to $\Delta=12°$ followed by a fairly sharp transition to 8.7 to 8.8 km/sec implies a velocity structure similar to that of the CIT11CS3 model down to the depth of 150 km. The small amplitude of the first arrival at $\Delta=14°$ implies that the velocity gradient at depths corresponding to $\Delta=14°$ is almost "critical". Under this condition the amplitude behavior becomes very sensitive to the velocity structure. Even a slight difference in velocity may cause a drastic change in the amplitude variation with distance. Although the lack of clear shadow zones excludes the possibility of a pronounced low-velocity layer, it is by no means unreasonable to assume a slight low-velocity zone. *Gutenberg* [1953, 1959] used the "minimum apparent velocity method" and found relatively low velocities of 7.7 to 7.9 km/sec at depths 50 to 150 km for some Japanese earthquakes. Although his method is not strictly valid when the rate of the velocity decrease is larger than the critical value, it is approximately valid for a low-velocity layer of smaller magnitude. In view of these we provisionally introduce a slight low-velocity layer at depths from 85 to 150 km

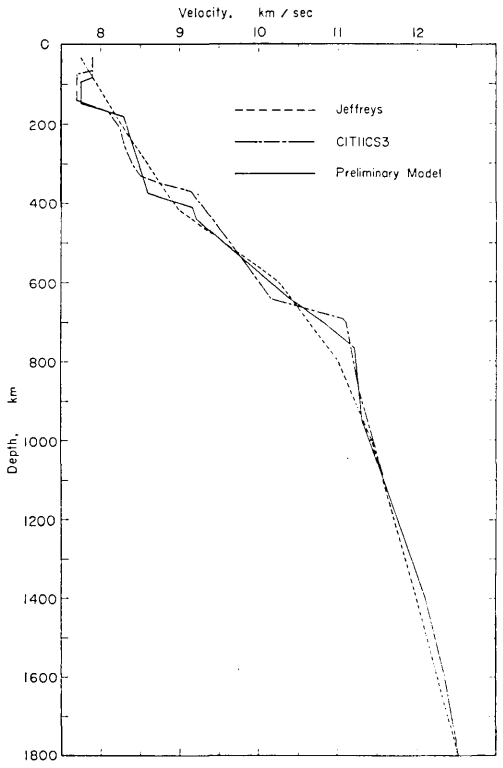


Fig. 13. Three velocity models. The preliminary model is constructed by modifying the Jeffreys and CIT11CS3 models such that it fits the observed apparent velocity data.

as shown in Figure 13. It should be noted that the regional difference is probably too large to justify a construction of a detailed model for this depth. The model given in Figure 13 should be taken as representing an approximate feature of the upper mantle structure around Japan. What is essential here is the relative constancy of the velocity to the depth of about 150 km.

The observed apparent velocity of 8.7 to 8.8 km/sec over the distance range $16° < \Delta < 19°$ is slightly higher than that for the CIT11CS3 model. The velocity values corresponding to this part of the apparent velocity curve are therefore slightly increased compared with those of the CIT11CS3 model but with an almost identical velocity gradient with depth (see Figure 13). The sharp discontinuity of the apparent velocity observed at $\Delta = 19.3°$ can be interpreted either in terms of a change in the velocity gradient alone or of a rapid change in velocity. We will take the latter possibility in order to explain the observed later phase branch which apparently forms a cusp at $\Delta = 15°$. The depth of this sharp increase in velocity is adjusted so as to place the discontinuity in the apparent velocity around $\Delta = 19.3°$. The sharpness and the amount of velocity increase are mainly determined by the general feature of the later phase branch but also by the behavior of the apparent velocity increase from $\Delta = 19.5°$ to 23°. The observed variation of the apparent velocity with distance for $19.5° < \Delta < 23°$ lies midway between the Jeffreys and the CIT11CS3 models. Thus we constructed a velocity-depth function corresponding to this portion of the apparent velocity curve such that it has a rapid increase at the depth

Table 2. Velocity-depth structures for three models.

| JEFFREYS | | | CIT11CS3 | | | PRELIMINARY MODEL | | |
|---|---|---|---|---|---|---|---|---|
| DEPTH (KM) | RADIUS (KM) | VELOCITY (KM/SEC) | DEPTH (KM) | RADIUS (KM) | VELOCITY (KM/SEC) | DEPTH (KM) | RADIUS (KM) | VELOCITY (KM/SEC) |
| 0 | 6371 | 5.57 | 0 | 6371 | 5.57 | 0 | 6371 | 5.57 |
| 15 | 6356 | 5.57 | 15 | 6356 | 5.57 | 15 | 6356 | 5.57 |
| 15 | 6356 | 6.50 | 15 | 6356 | 6.50 | 15 | 6356 | 6.50 |
| 33 | 6338 | 6.50 | 33 | 6338 | 6.50 | 33 | 6338 | 6.50 |
| 33 | 6338 | 7.75 | 33 | 6338 | 7.90 | 33 | 6338 | 7.90 |
| 100 | 6271 | 7.95 | 65 | 6306 | 7.90 | 85 | 6286 | 7.90 |
| 200 | 6171 | 8.26 | 75 | 6296 | 7.70 | 95 | 6276 | 7.75 |
| 300 | 6071 | 8.58 | 140 | 6231 | 7.70 | 150 | 6221 | 7.75 |
| 413 | 5958 | 8.97 | 170 | 6201 | 8.10 | 180 | 6191 | 8.27 |
| 600 | 5771 | 10.25 | 210 | 6161 | 8.25 | 250 | 6121 | 8.40 |
| 800 | 5571 | 11.00 | 250 | 6121 | 8.30 | 375 | 5996 | 8.60 |
| 1000 | 5371 | 11.42 | 300 | 6071 | 8.40 | 410 | 5961 | 9.15 |
| 1200 | 5171 | 11.71 | 330 | 6041 | 8.50 | 440 | 5931 | 9.20 |
| 1400 | 4971 | 11.99 | 350 | 6021 | 8.75 | 540 | 5831 | 9.77 |
| 1600 | 4771 | 12.26 | 370 | 6001 | 9.15 | 640 | 5731 | 10.35 |
| 1800 | 4571 | 12.53 | 450 | 5921 | 9.45 | 700 | 5671 | 10.80 |
| 2000 | 4371 | 12.79 | 500 | 5871 | 9.65 | 765 | 5606 | 11.20 |
| 2200 | 4171 | 13.03 | 600 | 5771 | 10.00 | 950 | 5421 | 11.30 |
| 2400 | 3971 | 13.27 | 640 | 5731 | 10.15 | 1400 | 4971 | 12.10 |
| 2600 | 3771 | 13.50 | 665 | 5706 | 10.55 | 1600 | 4771 | 12.35 |
| 2800 | 3571 | 13.64 | 690 | 5681 | 11.05 | 1800 | 4571 | 12.53 |
| 2898 | 3473 | 13.64 | 700 | 5671 | 11.10 | 2000 | 4371 | 12.79 |
| | | | 800 | 5571 | 11.20 | 2200 | 4171 | 13.03 |
| | | | 900 | 5471 | 11.30 | 2400 | 3971 | 13.27 |
| | | | 1000 | 5371 | 11.45 | 2600 | 3771 | 13.50 |
| | | | 1200 | 5171 | 11.71 | 2800 | 3571 | 13.64 |
| | | | 1400 | 4971 | 11.99 | 2898 | 3473 | 13.64 |
| | | | 1600 | 4771 | 12.26 | | | |
| | | | 1800 | 4571 | 12.53 | | | |
| | | | 2000 | 4371 | 12.79 | | | |
| | | | 2200 | 4171 | 13.03 | | | |
| | | | 2400 | 3971 | 13.27 | | | |
| | | | 2600 | 3771 | 13.50 | | | |
| | | | 2800 | 3571 | 13.64 | | | |
| | | | 2898 | 3473 | 13.64 | | | |

of 375 km followed by a gradual increase with a slope between that of the Jeffreys and the CIT11CS3 models. From $\Delta=27°$ to 40° the apparent velocity is fairly constant around 12.8 to 13 km/sec. This means that the velocity at depths corresponding to this distance range is relatively constant and about 15 per cent less than the apparent velocity since the depth is about 15 per cent of the earth's radius. Although no data are available around $\Delta=25°$, it is evident that the increase of the apparent velocity from $\Delta=23°$ to 27° is rapid. Combining this with the constancy of the apparent velocity at $27°<\Delta<40°$ we constructed a velocity model which has a slightly rapid increase from 640 to 770 km followed by an almost constant velocity down to 950 km. The velocity variation at 640 km can be sharper than that indicated in Figure 13, but a more gradual variation would not be consistent with the observed apparent velocity. At distances larger than 43°, there is an indication that the apparent velocity again starts increasing, although the apparent velocity measurement becomes less reliable. The velocity structure for this portion is constructed so as to fit the observed apparent velocity only

in an approximate manner. The entire velocity-depth model thus constructed is shown in Figure 13 and Table 2. The corresponding travel times and apparent velocities are shown in Figures 12 and 14 respectively. The fit of the apparent velocity curve to the observed data is generally good, and the travel-time curve explains the observed times satisfactorily.

The overall feature of the model constructed here has an intermediate character between the Jeffreys and the CIT11CS3 models.

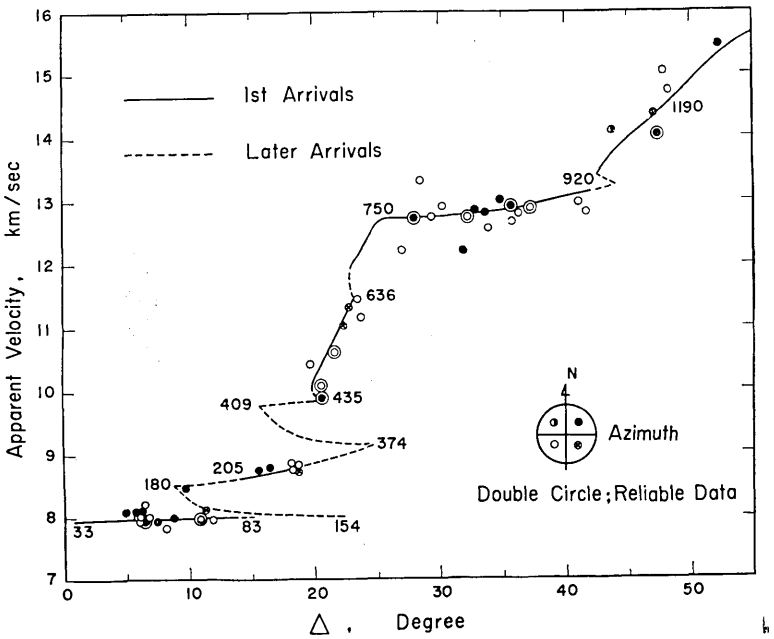


Fig. 14. Observed apparent velocities as compared with the calculated curve for the preliminary model given in Figure 13. Solid and dotted segments correspond to the first and later arrivals respectively. Numbers indicate the depth of penetration.

## § 6. Discussion

The approximate constancy of the apparent velocity up to $\Delta=12°$ observed here may be compared to the findings by *Dahm* [1936], *Lehmann* [1955], *Jeffreys* [1954], and *Cleary and Doyle* [1962] who reported that, in some regions, the travel-time curve is nearly straight up to about 14° to 15°. *Jeffreys* [1966] gave a value of $7.870\pm0.024$ km/sec for the average apparent velocity over $2°<\Delta<10°$ for Japanese earthquakes.

From a study of Hindu Kush earthquakes, *Shirokova* [1959] reported a rather rapid velocity increase from 8.00 to 8.71 km/sec at the depth from 40 to 100 km. No indication of the velocity increase of this sort is found in the present work.

*Dahm* [1936], and *Lehmann* [1959, 1962] placed a rapid or discontinuous velocity increase at a depth slightly larger than 200 km. The rapid increase of the velocity is found here at a depth slightly less than 200 km.

The 8.6 km/sec branch found here may correspond to that reported by *Ryall* [1962] who found a branch of 8.9 km/sec velocity from $\Delta=12°$ to 19°. *Archambeau et al.* [1966], and *Roller and Jackson* [1966] have also found a branch with 8.5 to 8.6 km/sec velocity which emerges at distances around $\Delta=12°$. The abrupt increase at around 19° has been frequently reported since *Byerly* [1926] found it for the Montana earthquake of 1925. *Archambeau et al.* [1966] also found this discontinuity at about 19° for the Salmon experiment. *Doyle and Webb* [1963], *Golenetskii and Medvedeva* [1965], *Niazi and Anderson* [1965] found an indication of the discontinuous change in $d\Delta/dt$ at $\Delta=16.5°$ to 17° rather than at 19°.

Niazi and Anderson also reported another discontinuity at $\Delta=24°$. No data are available here around this distance but a relatively rapid increase is indicated.

The observed constancy of the apparent velocities over $27°<\Delta<40°$ is consistent with the findings by *Ryall* [1962], and *Doyle and Webb* [1963] who reported that the travel-time curve is straight with a slope of 12.5 to 12.6 km/sec over $25°<\Delta<40°$.

Recently *Johnson* [1967] measured $dt/d\Delta$ at Tonto Forest, Arizona, for both first and later arrivals. His $dt/d\Delta$ results at $\Delta<22°$ are in close agreement with the present results and therefore his velocity structure (CIT204) is very similar to the present model (Figure 13) above 500 km.

Although many of the features found here are consistent with those of previous works as mentioned above, a number of disagreements are also noticed. Since the data used here are only from a six-month observation, the present result should be regarded as preliminary. It is hoped in future studies to triple the amount of data and combine more quantitative later phase and amplitude observations to attain the uniqueness of the solution which is hardly obtainable with the present amount of data.

The construction of the velocity-depth function is based primarily on the $d\Delta/dt$ curve without direct reference to travel times. It is interesting to compare the travel times for the preliminary model given in Figure 13 with those recently reported. Figure 15 shows the travel time residuals from the Jeffreys-Bullen times as compared with those of three nuclear explosions [*Gordon*, 1966] and a number of earthquakes observed in the United States [*Cleary and Hales*, 1966]. The position of the base line is different for different events. This is partly due to structural differences of the source area. Aside from the shift of the base line which is adjustable by shallower structures, the general trend of the travel time curve for the preliminary model is quite similar to others over the distance range $25° < \Delta < 60°$. This implies that the modification of the Jeffreys model in the manner shown in Figure 13 for the depth range of 600 to 1800 km is one of the possible solutions which explain the recently reported residuals from the J-B Table.

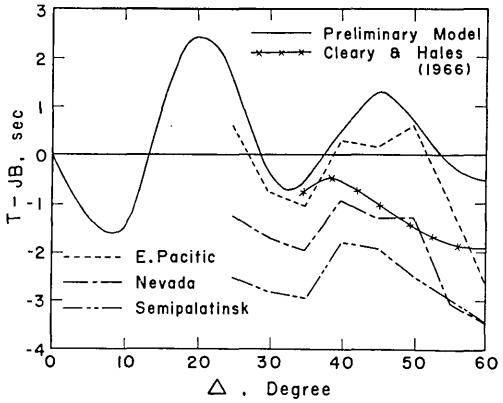


Fig. 15. Travel time residual from the J-B Table calculated for the preliminary model given in Figure 13 as compared with those for three explosions and that for earthquakes.

*Ludwig et al.* [1966] reported $P_n$ velocities of 8.0 to 8.3 km/sec near the Japan trench. Since no earthquakes of $\Delta < 5°$ are used in the present analysis it is not possible to determine the velocity just below the Moho discontinuity. In the ocean explosion studies, however, it is not possible to determine deeper structures, since the depth of the wave penetration is very shallow. The relatively high $P_n$ velocities observed by Ludwig *et al.* and the relatively low upper mantle velocity inferred by the present work can be reconciled if we consider the possibility that the velocity just below the oceanic Moho may be large compared with that further below due presumably to the temperature effect.

Figure 16 shows the preliminary velocity model as compared with distributions of earthquake energy release in Japan region [*Gutenberg*, 1957; *Miyamura*, 1966; *Mizoue*, 1967], a phase diagram of the olivine-spinel transition [*Akimoto and Fujisawa*, 1966, 1967], temperature

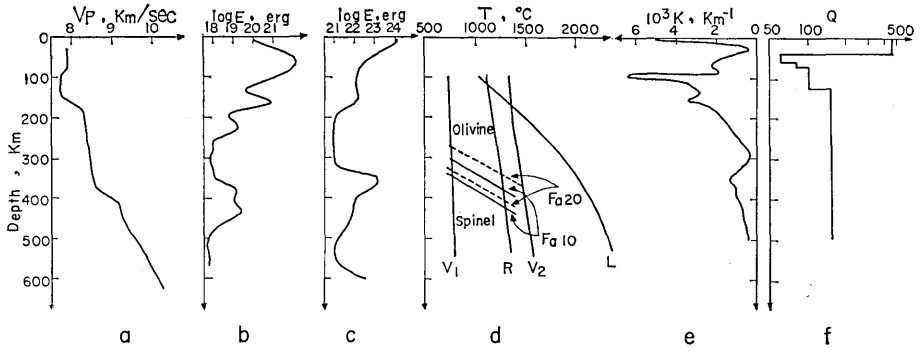


Fig. 16. The velocity-depth model (a), earthquake energy release (b, c), olivine-spinel phase diagram (d), temperature distributions (d), attenuation coefficient (e), and $Q$ (f). The earthquake energy curve (b) is recalculated from the data given by *Miyamura* [1966], and *Mizoue* [1967]. The total energies released for the period January 1963 to June 1966 in their regions 18 and 19 are averaged. Figure c is the annual energy release calculated by *Gutenberg* [1957]. Sources of the temperature distributions in (d) are as follows.

$V_1$, $V_2$: *Verhoogen* [1954]
R: *Rikitake* [1952]
L: *Lubimova* [1958]

The olivine-spinel phase diagrams are from *Akimoto and Fujisawa* [1967].

distributions [*Verhoogen*, 1954; *Rikitake*, 1952; *Lubimova*, 1958], a distribution of attenuation coefficient [*Wadati and Hirono*, 1956], and a distribution of $Q$ [*Anderson et al.*, 1965].

The minimum of $\log E$ at the depth of 140 km may correspond to the low-velocity layer as suggested by *Gutenberg* [1957]. This depth also approximately coincides with the level of maximum attenuation suggested by Wadati and Hirono, and also with the trough of the $Q$ distribution of Anderson *et al.* A common cause of this coincidence is most probably a temperature effect. A more quantitative discussion is highly desirable on the basis of more quantitative data. The maximum of the energy release at the depth of 170 km (Figure 16) corresponds to the sharp increase of velocity at the same depth. *Johnson* [1967] also found a relatively rapid increase in velocity near a depth of 160 km. The rate of the velocity increase at this level can hardly be explained by the simple pressure effect alone. If the cause of the low-velocity layer is a simple temperature effect, compositional change may be required to explain this rapid change in velocity. On the other hand, if the low-velocity layer is a seismological manifestation of partial meltings, this rapid increase is probably due to "rehardening" of the material caused by a downward separation of the temperature distribu-

tion from the melting curve. The latter view may be more favorable to the observed increase of the earthquake energy release, but the question is still open.

The marked increase in velocity starting at the depth of 375 km is one of the features which are commonly referred to as the 20° discontinuity. The existence of this marked velocity increase has also been verified by several recent works [*Niazi and Anderson*, 1965; *Anderson and Julian*, 1965; *Archambeau et al.*, 1966; *Johnson*, 1967; *Archambeau and Flinn*, 1967]. The possible relation of the 20° discontinuity to the phase transition of the mantle material has been frequently discussed, among others, by *Jeffreys* [1937] and *Birch* [1952], and recently detailed discussions were made by *Sclar et al.* [1964], *Anderson* [1965, 1967*a*, 1967*b*], *Ringwood* [1966], and *Fujisawa* [1966, 1967]. If the velocity increase is due to the olivine-spinel transition, we can estimate the temperature at this level with relatively small uncertainties by collating the phase diagram (Figure 16d) with the velocity distribution (Figure 16a). From Figure 16, the temperature can be estimated as 1500°C and 1300°C at the depth of 375 km corresponding to a mantle model consisting of $(Mg_{0.8}Fe_{0.2})_2SiO_4$ and $(Mg_{0.9}Fe_{0.1})_2SiO_4$ olivine respectively. This temperature falls between the minimum and maximum temperatures suggested by *Verhoogen* [1954] and is in the same neighborhood of that determined by *Rikitake* [1952] from electrical conductivity studies. The temperature distribution based on thermal history calculations [*Lubimova*, 1958] is also shown in Figure 16d. It gives much higher temperatures compared with those by Verhoogen and Rikitake. If the mantle mainly consists of magnesium olivines and the pressure scale used for the construction of the olivine-spinel phase diagram is correct, this temperature distribution is not compatible, at least around Japan, with the idea of correlating the rapid velocity increase at the depth of 375 km to the phase transition. *Anderson* [1967*b*] interprets this rapid velocity change in terms of the olivine-spinel transition of $Mg_2SiO_4-Fe_2SiO_4$ system with an increasing fayalite content with depth. A marked peak of the earthquake energy release at the same depth is suggestive of the common cause. This peak is notable only in the Japan region. The idea of correlating the phase transition to the peak of the strain release is that the level of the phase transition has a potential capability of converting thermal energy to mechanical energy through the volume change associated with the phase transition. Although the mantle at about 400 km depth has the potential capability, no strain accumulation and therefore no

strain release occur unless thermal energy is supplied. The notable strain release at this depth observed only in the Japan region implies that the temperature at this depth is still changing and some mechanism is operative to transfer the thermal energy. The lack of a notable strain release at this level in other regions in the world may imply that the temperature at the level either has been stabilized or has not as yet been agitated. All of these ideas are highly speculative but future works on earthquake source mechanisms and seismicity in relation to the mantle structure may solve the problem.

The velocity structure derived here is slightly different from *Johnson's* [1967] CIT204 and the CIT109P by *Archambeau and Flinn* [1967] at depths 450 to 600 km. Although some complicated features were observed in seismograms, it was not possible to identify a clear later phase branch in the present study. The present velocity model should therefore be regarded as a somewhat smoothed version of the actual structure over this depth range. Since the earth's mantle probably consists of olivines and pyroxenes, we may expect a series of phase transitions such as $Mg_2SiO_4$ (spinel)$\rightarrow MgSiO_3$ (ilmenite)$+MgO$, $MgSiO_3$ (ilmenite)$\rightarrow MgO+SiO_2$ (stishovite), $2MgSiO_3$ (enstatite)$\rightarrow Mg_2SiO_4$ (spinel)$+SiO_2$ (stishovite), and other pyroxene transformations. It is therefore possible that the apparently gradual increase of velocity of the present model at 450 to 700 km may represent successive stepwise variations. Unfortunately, none of the transitions listed above has been experimentally verified and the present determination of the structure at these depths is not accurate enough to justify detailed discussions. The revision of the structure below 450 km must await future studies including detailed later phase and amplitude analyses.

## Acknowledgments

I am indebted to Dr. Setumi Miyamura and Mr. Kenshiro Tsumura for the use of facilities and seismograms at Wakayama Micro-Earthquake Observatory. I thank Drs. Syun-iti Akimoto, Hideyuki Fujisawa, and Megumi Mizoue for allowing me to use the results of their recent works before publication. I also wish to thank Drs. Don Anderson and Lane Johnson for giving me valuable suggestions and sending me the preprints. I am grateful to Drs. Frank Press and Keiiti Aki, who kindly read the manuscript and gave me various comments. The preparation of the manuscript and diagrams was assisted by Miss T. Hirasawa, and the

computations were carried out at the Computer Center of the University of Tokyo.

## References

AKIMOTO, S., and H. FUJISAWA, Olivine-spinel transition in the system $Mg_2SiO_4$–$Fe_2SiO_4$ at 800°C, *Earth and Planetary Science Letters*, **1**, 237-240, 1966.

AKIMOTO, S., and H. FUJISAWA, Olivine-spinel solid solution equilibria in the system $Mg_2SiO_4$–$Fe_2SiO_4$, *J. Geophys. Res.*, in preparation, 1967.

ANDERSON, Don L., Recent evidence concerning the structure and composition of the earth's mantle, *Phys. Chem. Earth*, **6**, 1-131, 1965.

ANDERSON, Don L., Latest information from seismic observations, in *The Earth's Mantle*, edited by T. F. Gaskell, Academic Press, London, 1967*a*.

ANDERSON, Don L., Phase changes in the upper mantle, preprint, 1967*b*.

ANDERSON, Don L., A. BEN-MENAHEM, and C. B. ARCHAMBEAU, Attenuation of seismic energy in the upper mantle, *J. Geophys. Res.*, **70**, 1441-1448, 1965.

ANDERSON, Don L., and B. JULIAN, Travel times, apparent velocities, and amplitudes of body waves, presented at Seismological Society of America, 1965 Annual meeting St. Louis, see *Anderson* [1967*a*].

ANDERSON, Don L., and M. N. TOKSÖZ, Surface waves on a spherical earth, 1. Upper mantle structure from Love waves, *J. Geophys. Res.*, **68**, 3483-3499, 1963.

ARCHAMBEAU, C. B., E. A. FLINN, and D. G. LAMBERT, Detection, analysis, and interpretation of teleseismic signals, 1. Compressional phases from the Salmon event, *J. Geophys. Res.*, **71**, 3483-3501, 1966.

ARCHAMBEAU, C. B., and E. A. FLINN, in preparation, see *Anderson* [1967*b*].

BIRCH, F., Elasticity and constitution of the earth's interior, *J. Geophys. Res.*, **57**, 227-286, 1952.

BYERLY, P., The Montana earthquake of June 28, 1925, *Bull. Seismol. Soc. Am.*, **16**, 209-265, 1926.

CHINNERY, M. A., and M. N. TOKSÖZ, *P*-wave velocities in the mantle below 700 km, *Bull. Seismol. Soc. Am.*, **57**, 199-226, 1967.

CLEARY, J., and H. DOYLE, Application of a seismograph network and electronic computer in near earthquake studies, *Bull. Seismol. Soc. Am.*, **52**, 673-682, 1962.

CLEARY, J., and A. L. HALES, An analysis of the travel times of *P* waves to North American stations in the distance range 32° to 100°, *Bull. Seismol. Soc. Am.*, **56**, 467-489, 1966.

DAHM, C. G., Velocities of *P* and *S* waves calculated from the observed travel times of the Long Beach earthquake, *Bull. Seismol. Soc. Am.*, **26**, 159-171, 1936.

DOYLE, H. A., and J. P. WEBB, Travel times to Australian stations from Pacific nuclear explosions in 1958, *J. Geophys. Res.*, **68**, 1115-1120, 1963.

FUJISAWA, H., Olivines under high pressures and high temperatures, Thesis, Geophysical Institute, University of Tokyo, 1966.

FUJISAWA, H., Temperature and discontinuities in the transition layer within the earth's mantle: Geophysical application of olivine-spinel transition in the system $Mg_2SiO_4$–$Fe_2SiO_4$, in preparation, 1967.

GOLENETSKIĬ, S. I., and G. Ya. MEDVEDEVA, On discontinuities of the first kind in the earth's upper mantle, *Bull. Acad. Sci. USSR, Geophys. Ser., English Transl.*, 318-322, 1965.

GORDON, D. W., Travel time curve, ESSA symposium on earthquake prediction, February 1966, pp. 141-145, published by U.S. Department of Commerce, 1966.

GUTENBERG, B., Wave velocities at depths between 50 and 600 kilometers, *Bull. Seismol. Soc. Am.*, **43**, 223-232, 1953.

GUTENBERG, B., Earthquake energy released at various depths, *Verhandel. Ned. Geol. Minigbouwk Gernoot., Geol. Ser.*, **18**, 165-175, 1957.

GUTENBERG, B., The asthenosphere low-velocity layer, *Ann. Geofis. Rome*, **12**, 439-460, 1959.

JEFFREYS, H., The structure of the earth down to the 20° discontinuity (second paper), *Monthly Notices Roy. Astron. Soc., Geophys. Suppl.*, **4**, 13-39, 1937.

JEFFREYS, H., The times of *P* in Japanese and European earthquakes, *Monthly Notices Roy. Astron. Soc., Geophys. Suppl.*, **6**, 557-565, 1954.

JEFFREYS, H., Revision of travel times, *Geophys. J.*, **11**, 5-12, 1966.

JOHNSON, L. R., Array measurements of *P* velocities in the upper mantle, *J. Geophys. Res.*, in preparation, 1967.

KISHIMOTO, Y., Seismometric investigation of the earth's interior, Part 3. On the structure of the earth's mantle (I), *Memoirs of the College of Science, University of Kyoto, Series A*, **28**, 117-142, 1956.

LEHMANN, I., The times of *P* and *S* in northeastern America, *Ann. Geofis. Rome*, **8**, 351-370, 1955.

LEHMANN, I., Velocities of longitudinal waves in the upper part of the earth's mantle, *Ann. Geophys.*, **15**, 93-118, 1959.

LEHMANN, I., The travel times of the longitudinal waves of the Logan and Blanca atomic explosions and their velocities in the upper mantle, *Bull. Seismol. Soc. Am.*, **52**, 519-526, 1962.

LUBIMOVA, E. A., Thermal history of the earth with consideration of the variable thermal conductivity of its mantle, *Geophys. J.*, **1**, 115-134, 1958.

LUDWIG, W. J., J. I. EWING, M. EWING, S. MURAUCHI, N. Den, S. ASANO, H. HOTTA, M. HAYAKAWA, T. ASANUMA, K. ICHIKAWA, and I. NOGUCHI, Sediments and structure of the Japan trench, *J. Geophys. Res.*, **71**, 2121-2137, 1966.

MIYAMURA, S., Seismicity of island arcs with different ages (abstract), *Proceedings of the 11th Pacific Science Congress*, **3**, 22, 1966.

MIZOUE, M., Variation of earthquake energy release with depth, *Bull. Earthquake Res. Inst. Tokyo Univ.*, **45**, to be published, 1967.

NIAZI, M., Corrections to apparent azimuths and travel-time gradients for a dipping Mohorovičić discontinuity, *Bull. Seismol. Soc. Am.*, **56**, 491-509, 1966.

NIAZI, M., and Don L. ANDERSON, Upper mantle structure of western North America from apparent velocities of *P* waves, *J. Geophys. Res.*, **70**, 4633-4640, 1965.

NUTTLI, O., Seismological evidence pertaining to the structure of the earth's upper mantle, *Rev. Geophys.*, **1**, 351-400, 1963.

RIKITAKE, T., Electrical conductivity and temperature in the earth, *Bull. Earthquake Res. Inst. Tokyo Univ.*, **30**, 13-24, 1952.

RINGWOOD, A. E., Mineralogy of the mantle, in *Advances in Earth Science*, edited by P. M. Hurley, pp. 357-399, MIT Press, Cambridge, 1966.

ROLLER, J. C., and W. H. JACKSON, Seismic wave propagation in the upper mantle: Lake Superior, Wisconsin, to central Arizona, *J. Geophys. Res.*, **71**, 5933-5941, 1966.

RYALL, A., The Hebgen Lake, Montana, earthquake of August 18, 1959: *P* waves, *Bull. Seismol. Soc. Am.*, **52**, 235-271, 1962.

SAVARENSKII, E. F., Investigation of the upper mantle of the earth by seismic body waves, *Bull. Acad. Sci. USSR, Geophys. Ser., English Transl.*, 133-140, 1966.

SCLAR, C. B., L. C. CARRISON, and C. M. SCHWARTZ, High-pressure reaction of clinoenstatite to forsterite plus stishovite, *J. Geophys. Res.*, **69**, 325-330, 1964.

SHIROKOVA, E. I., Some facts on the character of the velocity change in the upper layers of the earth's mantle, *Bull. Acad. Sci. USSR, Geophys. Ser., English Transl.*, 804-813, 1959.

VERHOOGEN, J., Petrological evidence on temperature distribution in the mantle of the earth, *Trans. Am. Geophys. Union*, **35**, 85-92, 1954.

WADATI, K., T. HIRONO, Magnitude of earthquake—Especially of near, deep-focus earthquakes, *Geophysical Magazine*, **27**, 1-10, 1956.

WAKAYAMA MICRO-EARTHQUAKE OBSERVATORY, Seismological bulletin of Wakayama micro-earthquake observatory and its substations, January-June, 1965, pp. 1-113, published by Wakayama Micro-Earthquake Observatory, Earthquake Research Institute, The University of Tokyo, Wakayama, 1966.

---

## 35. 和歌山微小地震観測所で観測された $P$ 波のみかけの速さとマントル上部の構造

地震研究所　金森博雄

1965年1月から6月の間に和歌山微小地震観測所網で観測された $P$ 波のみかけの速さ，$C$，を調べた．用いた地震は和歌山からの距離 $5° < \Delta < 55°$ のもので，次の結果が得られた．

距離 $5° < \Delta < 12°$ で $C \fallingdotseq 8$ km/sec, $15° < \Delta < 19°$ で $C \fallingdotseq 8.8$ km/sec, $19.5° < \Delta < 23.5°$ で $C$ は約 10 から 11.4 km/sec まで急増する．$25° < \Delta < 40°$ の間では $C \fallingdotseq 12.8 \sim 13.0$ km/sec で 43° 位から再びやや急に増加する．Jeffreys の $Vp$ モデルは観測されたみかけの速さをよく説明しない．観測結果をよく説明するモデルは次の通りである．深さ $d=33$ km から $d=160$ km まで，$Vp$ は約 7.9 km/sec でほぼ一定で，低速度層は 100 km～150 km までにごく小規模なものがあつてもよい．その他 Jeffreys のモデルと異なる点は，深さ 375 km から約 450 km と 640 km から 760 km の所で $Vp$ が急増することである．

また深さ 1000 km 位の所にも不確実ではあるが，$Vp$ の急増がみられる．これらはオリビン→スピネル，スピネル→イルメナイト＋ペリクレース，イルメナイト→ペリクレース＋スティショバイト転移と関係するものと思われる．また日本付近の地震活動の深さについての分布のピークは丁度 $d=375$ km と 450 km の間にある．このことは相転移と $Vp$ の急増と，地震の発生とが密接な関係にあることを示す．